HTML ABSTRACT • LINKS

Microstructure and properties of single crystal $BaTiO_3$ thin films synthesized by ion implantation-induced layer transfer

Young-Bae Park,[a] Jennifer L. Ruglovsky, and Harry A. Atwater
Thomas J. Watson Laboratory of Applied Physics, California Institute of Technology, Pasadena, California 91125

(Received 26 January 2004; accepted 25 May 2004)

Single crystal $BaTiO_3$ thin films have been transferred onto Pt-coated and Si_3N_4-coated substrates by the ion implantation-induced layer transfer method using H^+ and He^+ ion coimplantation and subsequent annealing. The transferred $BaTiO_3$ films are single crystalline with root mean square roughness of 17 nm. Polarized optical and piezoresponse force microscopy (PFM) indicate that the $BaTiO_3$ film domain structure closely resembles that of bulk tetragonal $BaTiO_3$ and atomic force microscopy shows a 90° $a-c$ domain structure with a tetragonal angle of 0.5°–0.6°. Micro-Raman spectroscopy indicates that the local mode intensity is degraded in implanted $BaTiO_3$ but recovers during anneals above the Curie temperature. The piezoelectric coefficient, d_{33}, is estimated from PFM to be 80–100 pm/V and the coercive electric field (E_c) is 12–20 kV/cm, comparable to those in single crystal $BaTiO_3$. © *2004 American Institute of Physics*. [DOI: 10.1063/1.1773373]

Ferroelectric thin films have been widely explored for application as capacitor dielectrics and memory elements in nonvolatile random access memory (NVRAM) devices, and have promise for high work/volume mechanical actuators in microelectromechanical systems (MEMS) applications.[1,2] In most cases, these ferroelectric thin films have a polycrystalline microstructure that degrades the piezoelectric coefficients, saturation polarization, and charge retention and causes time-dependent fatigue problems.

A number of film deposition methods have been studied to fabricate high quality ferroelectric oxides. Metalorganic chemical vapor deposition (MOCVD), molecular beam epitaxy (MBE), pulsed laser deposition (PLD) and sol–gel synthesis processes have been used for heteroepitaxial growth of ferroelectric thin films on various substrates.[3–6] However, in spite of many efforts to realize epitaxial growth on various lattice mismatched substrates, deposited thin films rarely exhibit properties comparable to those of bulk single crystals.

Layer transfer is one of the most promising methods by which to realize single crystal properties in thin films and to overcome substrate–film lattice mismatch effects. Crystal ion slicing (CIS) processes have been reported for layer transfer of silicon, InP, Ge and diamond.[7,8] Recently, layer splitting and transfer of ferroelectric materials such as $LiNbO_3$, $LiTaO_3$, $KTaO_3$, $SrTiO_3$, and $BaTiO_3$ by sacrificial wet etching and anodic bonding methods combined with the CIS method have also been reported.[9,10] To date, characterization of both the microstructure and ferroelectric properties of transferred ferroelectric thin films as well as the principal role of the implanted gas species have not been extensively reported. Single crystal ferroelectric thin films can be used in applications such as actuator devices, monolithically integrated optical waveguides on Si-based microelectronics devices and single domain capacitors. In this study, we have performed single crystal thin film layer transfer via H^+/He^+ coimplantation of single crystal $BaTiO_3$ with no subsequent chemical etching. Also, the ferroelectric, microstructural and electrical properties of the transferred layer have been investigated.

Ion implantation-induced layer transfer was performed on bulk single crystal $BaTiO_3$ [double side polished, (001) orientation, 5 mm × 5 mm × 1 mm]. H^+ and He^+ coimplantation was used for enhancement of cavity nucleation and growth via chemical and physical damage. During implantation, $BaTiO_3$ crystals were mounted on a 4 in. Si wafer. An Al foil mask allowed sequential ion implantation with H^+ and He^+ ions. The H^+ ion implantation energy was varied in the range of 20–80 keV with a dose of 5×10^{16}–$1\times10^{17}/cm^2$, and 30–115 keV He^+ ion was subsequently implanted with a dose in the range of 5×10^{16}–$1\times10^{17}/cm^2$. Implantation was performed at −25 °C to prevent the formation of cavities during implantation. The root mean square (rms) roughness of the surface was 2.0 nm for unimplanted bulk $BaTiO_3$ and 2.0–3.0 nm for as-implanted $BaTiO_3$. The substrates used for layer transfer were 50 nm thick low pressure CVD (LPCVD) grown Si_3N_4/n-Si with a surface roughness of 0.5–0.8 nm and 200 nm thick sputter-deposited Pt films on 50 nm Si_3N_4/Si with a surface roughness of 3.0 nm.

After the implantation step, both $BaTiO_3$ and the substrates were cleaned by dipping in methanol/acetone/deionized water to remove particles on the surfaces. The $BaTiO_3$ and substrates were bonded at room temperature and postbond annealing for layer splitting was performed either in a furnace in air ambient or a custom-designed wafer bonder in N_2 gas ambient from 300 to 500 °C for 0.5–24 h under pressure less than 2 MPa. In conjunction with the present layer transfer experiments, we also performed an investigation of the formation of blisters of unbonded but implanted $BaTiO_3$ during annealing, which yielded information on the hydrogen gas release and cavity formation kinetics during the initial stages of layer splitting. Details of this kinetics study will be published elsewhere.

Polarized optical microscopy, atomic force microscopy (AFM) and focused ion beam milling combined with scanning electron microscopy (SEM) were used to image the cavity morphology and distribution. Micro-Raman spectroscopy with a pump intensity of 16 mW/cm^2 was used to probe

[a]Author to whom correspondence should be addressed; electronic mail: ypark@caltech.edu

 © 2004 American Institute of Physics
Downloaded 14 Dec 2005 to 131.215.225.171. Redistribution subject to AIP license or copyright, see http://apl.aip.org/apl/copyright.jsp

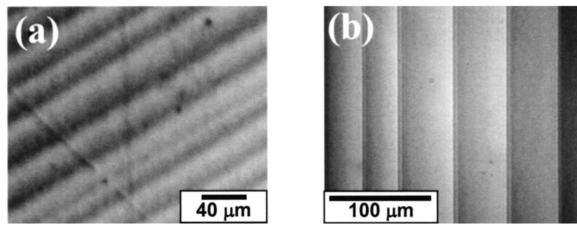

FIG. 1. Polarized optical microscopy images of (a) the transferred layer on a Pt-coated /Si substrate and (b) a bulk $BaTiO_3$ crystal.

local vibrational modes in implanted and annealed $BaTiO_3$.[11] Piezoresponse force microscopy (PFM) was used to investigate the ferroelectric domain structure. Probe tips were highly n-doped Si or Co-coated Si tips and the bias voltage, V_{ac}, was in the range of 1–5 V with frequency of 3–20 kHz, and the sample dc bias voltage was varied between −10 and 10 V.[12] Plan view transmission electron microscopy (TEM) analysis of freestanding films mounted on carbon grids was conducted at 200 kV accelerating voltage.

From observation of cavity formation prior to layer transfer, the mechanism for film transfer is determined to be macroscopic crack extension along the film–substrate interface as cavities coalesce. Coalescence between neighboring cavities is observed and Ostwald-type ripening is seen to be the dominant cavity growth mechanism.[13] This mechanism, driven by increases in the partial pressure of hydrogen and helium in cavities and microvoids combined with the elastic energy of the solid in the vicinity of cracks, is similar to the layer transfer mechanism which has now been widely observed in semiconductor materials.[14]

Figure 1(a) is a polarized-optical micrograph illustrating the domain structure of a transferred $BaTiO_3$ layer on a Pt-coated substrate. The domain structure in the film is seen to be strikingly similar to that of the unimplanted bulk $BaTiO_3$ crystal. The transferred layer is 300–400 nm thick and the transferred area is 5 mm × 5 mm, limited only by the bulk crystal size. The thickness is slightly lower than that simulated using Monte Carlo simulation analysis (SRIM 2003)[15] in which the projected ion range is 450 nm but is substantially smaller than the straggle of the projected ion range ($\Delta Rp \sim 100$ nm). The rms roughness (Rq) of the transferred $BaTiO_3$ surface determined from AFM is 17.1 nm, which is higher than the surface roughness of the single crystal $BaTiO_3$ surface ($Rq=2$ nm).

In order to confirm the crystallinity of the transferred layer, we transferred $BaTiO_3$ thin film layers implanted with low implantation energy (20 keV) directly onto carbon-coated TEM grids as the handle substrate. The thin $BaTiO_3$ layer was transferred at 300 °C for 30 min and the transferred layer thickness was about 150 nm as inferred by comparing the energy dispersive x-ray (EDX) intensity with signals from other standard $BaTiO_3$ samples with various thicknesses. Figure 2(a) shows TEM images for a 10 μm × 4 μm transferred $BaTiO_3$ layer and the selected area diffraction (SAD) pattern. The SAD pattern clearly shows the tetragonal single crystalline feature (space group: Cv, point group: $Pmm4$) and lattice parameters obtained from SAD are $a=0.3994$ nm and $c=0.4003$ nm which correspond to those of tetragonal $BaTiO_3$ single crystal. However, double diffraction patterns, indicated by arrows near the main diffraction spots, are observed, indicative of defect structures such as

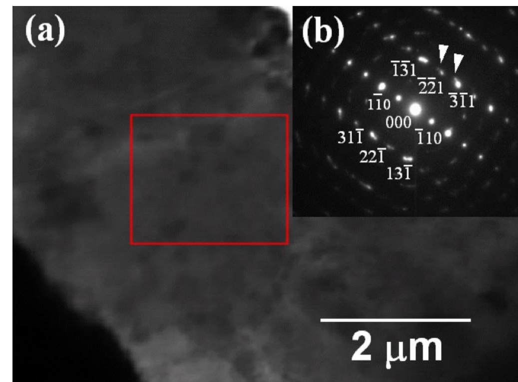

FIG. 2. (a) Plan view TEM image and (b) SAD pattern along the [114] zone axis for a 100 nm thick $BaTiO_3$ layer transferred onto a carbon coated grid. Ion implantation was performed at dose of 5×10^{16} ion/cm^2 for H^+ at an energy of 20 keV and 5×10^{16} ion/cm^2 for He^+ at energy of 30 keV, respectively.

twins or stacking faults, as well as local damage from ion implantation.

Raman spectroscopy shows the presence of tetragonal phase in $BaTiO_3$ by observation of the 305 cm^{-1} [full width at half maximum (FWHM)=4.6 cm^{-1}] and 710 cm^{-1} peaks.[11] These peaks are assigned to tetragonal $BaTiO_3$ and vanish above the Curie temperature ($T_C=120$°C). Thus the Raman results suggest that the crystal is tetragonal and in its ferroelectric state. Two broad bands centered at 272 and 513 cm^{-1} correspond to transverse optical (TO) phonons and their widths indicate large anharmonic coupling and a frequency dependent damping constant. The 272 and 513 cm^{-1} bands are observed in both cubic and tetragonal phase, although they are broader in cubic phase than in tetragonal phases. Following implantation, bulk $BaTiO_3$ crystals are damaged and show low Raman active mode intensities as shown in Fig. 3(b). However, annealing during the layer transfer process recovers the local mode intensities to levels comparable to those in the umimplanted bulk crystal as seen in Fig. 3(c). After layer transfer onto the substrate, the broad peak of the 200–400 cm^{-1} region, the absence of the sharp 305 cm^{-1} peak, and the broad 705 cm^{-1} peak in Fig. 3(c) suggest that the $BaTiO_3$ phase in this layer is imperfect due to large residual stress or local defects. Thus the transferred layer microstructure exhibits a bulk-like ferroelectric domain structure but has local crystallographic defects.

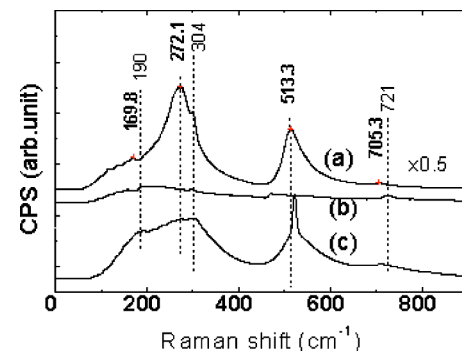

FIG. 3. Micro-Raman spectra of (a) annealed bulk $BaTiO_3$ after ion implantation at 300 °C for 30 min, (b) an as-implanted bulk $BaTiO_3$ crystal and (c) a transferred layer on the Si_3N_4(50 nm)/Si. The sharp peak at 520 cm^{-1} is due to the Si TO mode from the substrate.

Downloaded 14 Dec 2005 to 131.215.225.171. Redistribution subject to AIP license or copyright, see http://apl.aip.org/apl/copyright.jsp

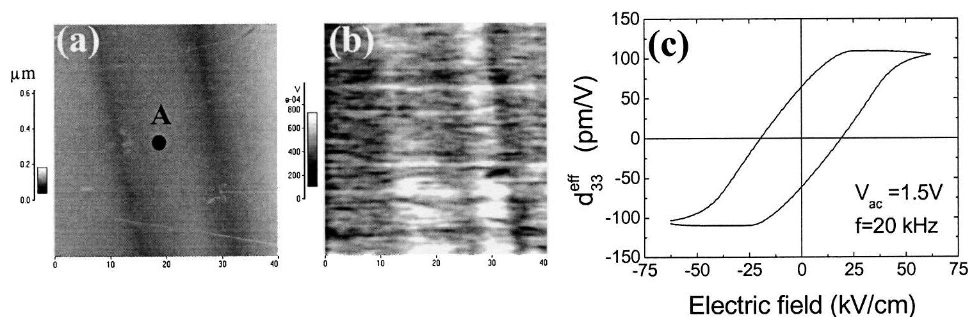

FIG. 4. Simultaneously obtained (a) AFM topographic and (b) PFM images of the transferred $BaTiO_3$ layer on Pt-coated Si and (c) piezoelectric hysteresis curve at point **A** in (a). The scanning area is 40 μm × 40 μm. The frequency and ac voltage applied on the AFM tip are 20 kHz and 1.5 V, respectively.

Figure 4 shows a typical AFM topographic image and a simultaneously acquired piezoresponse image of the transferred $BaTiO_3$ layer on the Pt/Si substrate of 40 μm × 40 μm. From the AFM and PFM images, it can be seen that the transferred film consists of 90° $a-c$ single domains with widths of 5–20 μm, which is a larger domain size than that typically reported for polycrystalline or epitaxial $BaTiO_3$ thin films. The domain structure as shown in Fig. 4(b) corresponds to the bulk $BaTiO_3$ structure in which tetragonal and rectangular shape domains have been observed.[10] The surface corrugation angle $[\Delta\theta = 90° \text{-} 2\arctan(a/c)]$ is 0.5–0.6° where a and c are lattice constants of the $BaTiO_3$ domain. In the piezoresponse image in Fig. 4(b), the bright and dark areas originate from contrast between in-plane and out-of plane oriented domains. From the dc bias applied between the conducting AFM tip and the substrate, the effective piezoelectric constant, d_{33}, value obtained is $\Delta Z = d_{33} V_{ac} \sin(\omega t)$ where Z is the longitudinal displacement, V_{ac} is the amplitude of the ac voltage and ω is frequency. d_{33} of the transferred $BaTiO_3$ thin film is in the range of 80–100 pm/V, depending on the domain position, at voltages under ±10 V. This d_{33} is smaller than that for bulk $BaTiO_3$ which has been reported as 190 pm/V.[16] The smaller d_{33} value is attributed to the clamping effect of the thick Si substrate in the case of transferred thin films. In addition, the measurement was performed without a domain poling process; the piezoelectric properties could be further improved with optimal poling.[17]

We obtained typical polarization field hysteresis curves, illustrated in Fig. 4(c), for a single ferroelectric domain (point A) by using the conducting AFM tip as the top electrode in PFM. The coercive electric field (E_c) at which the polarization changes its direction is 12–20 kV/cm and is smaller than typical E_c that ranged from 30 to 53 kV/cm in polycrystalline $BaTiO_3$.[6] The coercive field is known to be sensitive to the presence of defects and we note that the E_c of transferred $BaTiO_3$ thin films is comparable to that exhibited by single crystals (7–10 kV/cm),[18] indicating that the transferred $BaTiO_3$ layer shows nearly single crystal coercivity despite the presence of some domain-related defects.

This work was supported by the Army Research Office (ARO-MURI) under Grant No. DAAD 19-01-1-0517. One of the authors (Y.-B.P.) wishes to acknowledge support by the Postdoctoral Fellowship Program of the Korea Science and Engineering Foundation (KOSEF).

[1] A. I. Kingon, J. P. Maria, and S. K. Streiffer, Nature (London) **406**, 1032 (2000).
[2] D. L. Polla and L. F. Fraancis, Annu. Rev. Mater. Sci. **28**, 563 (1998).
[3] B. H. Hoerman, G. M. Ford, L. D. Kaufmann, and B. W. Wessles, Appl. Phys. Lett. **73**, 2248 (1998).
[4] D. G. Schlom, J. H. Haeni, J. Lettieri, C. D. Theis, W. Tian, J. C. Jiang, and X. Q. Pan, Mater. Sci. Eng., B **87**, 282 (2001).
[5] C. Li, Z. Chen, D. Lui, Y. Zhou, H. Lu, C. Dong, and H. Chen, J. Appl. Phys. **86**, 4555 (1999).
[6] H. B. Sharma and H. N. Sarma, Thin Solid Films **330**, 178 (1998).
[7] M. Bruel, Electron. Lett. **31**, 1201 (1995).
[8] Q. Y. Tong, K. Gutjahr, S. Hopfe, U. Gösele, and T. H. Lee, Appl. Phys. Lett. **70**, 1390 (1997).
[9] M. Levy, R. M. Osgood, R. Liu, L. E. Cross, G. S. Cargill, A. Kumer, and H. Bakhru, Appl. Phys. Lett. **73**, 2293 (1998).
[10] T. Izuhara, I. Gheorma, R. M. Osgood, A. N. Roy, H. Bakhru, Y. M. Tesfu, and M. E. Reeves, Appl. Phys. Lett. **82**, 616 (2003).
[11] L. H. Robins, D. L. Kaiser, L. D. Rotter, P. K. Schenck, G. T. Stauf, and D. Rytz, J. Appl. Phys. **76**, 7487 (1994).
[12] A. Gruverman, O. Auciello, and H. Tokumoto, Annu. Rev. Mater. Sci. **28**, 101 (1998); J. W. Hong, K. H. Noh, S.-I. Park, S. I. Kwon, and Z. G. Khim, Phys. Rev. B **58**, 5078 (1998).
[13] V. Raineri, M. Saggio, and E. Rimini, J. Mater. Res. **15**, 1449 (2000).
[14] L. J. Huang, Q. Y. Tong, Y. L. Caho, T. H. Lee, T. Martini, and U. Gösele, Appl. Phys. Lett. **74**, 982 (1999).
[15] J. F. Ziegler, J. P. Biersack, and U. Littmark, *The Stopping and Range of Ions in Solids* (Pergamon, New York, 1985).
[16] S. V. Kalinin and D. A. Bonnell, Phys. Rev. B **65**, 125408 (2002).
[17] Y. Wang, C. Ganpule, B. T. Liu, H. Li, K. Mori, B. Hill, M. Wuttig, R. Ramesh, J. Finder, Z. Yu, R. Droopad, and K. Eisenbeiser, Appl. Phys. Lett. **80**, 97 (2002).
[18] J. J. Urban, J. E. Spanier, L. Ouyang, W. S. Yun, and H. Park, Adv. Mater. (Weinheim, Ger.) **15**, 423 (2003).

Downloaded 14 Dec 2005 to 131.215.225.171. Redistribution subject to AIP license or copyright, see http://apl.aip.org/apl/copyright.jsp